

Space-Based Radar Polarimetry, Demythologized

R K Raney, 2kR-LLC

ABSTRACT

Ten fundamental polarimetric principles sufficient to characterize a quasi-monochromatic electro-magnetic field are presented. Although many of these may be familiar to readers, when collected together as an ordered set, they expose the inherent elegant simplicity that undergirds space-based radar polarimetry. Selected consequences are summarized. Appendices are included, one that reviews theoretical foundations that justify the claims made in the principles, and a second that briefly comments on traditional quad-pol radar polarimetry. The novel approach in Appendix I to normalization of polarimetric child parameters reveals simple proofs for several of the key principles.

1. Introduction

The polarization properties of a quasi-monochromatic electromagnetic field have been formally characterized for more than two centuries [Born and Wolf 1959, pp xx, xxi]. Pivotal theoretical progress was made during the 19th century [Fresnel 1821; Stokes 1852; Maxwell 1865; Poincaré 1892]. Popular textbooks explain and elaborate on that background [Jenkins and White 1957; Hecht 1987]. Polarimetric measurements have been central to advances in radio astronomy [Cohen 1958] and radar astronomy [Green 1968, Tinbergen 1996] among several other disciplines. Following four decades of elementary dual-polarized imaging radar remote sensing experience [Henderson and Lewis 1998, Ch 5], a fully-polarimetric imaging implementation was introduced for synthetic aperture radar (SAR) [vanZyl et al. 1987] which was a seismic-scale contribution.

Fully-polarimetric SAR—or, to use the common terminology, quad-pol SAR—requires measurement of all four Sinclair scattering matrix elements [Emmons and Alexander 1983]. From those data, mathematical methods are applied to retrieve polarimetric characterizations of the observed scene [Cloude and Potter 1996]. In spite of the impressive theoretical methodology and applications success of this technology, there are two unfortunate consequences: (1) The quad-pol SAR approach is perceived—incorrectly—by many in the broader professional community to be the only way to evaluate the full polarimetric characteristics of an observed scene [Raney 2021]; and (2) When implemented in a space-based system, the operational utility of data from a quad-pol SAR is seriously limited [Charbonneau et al. 2010, Brisco et al. 2020].

In contrast to the default quad-pol paradigm for space-based radar polarimetry, there is an alternative and much simpler approach based on fundamental principles that is well-suited to large-scale operational applications. After reading the opening sections of this paper, a knowledgeable person could be moved to observe—correctly—that most of these principles may be found (explicitly or implicitly) in the vast polarimetric literature. Those key principles—at least in the experience of this writer—never have been brought together as a compact

logical set. When so assembled, they reveal significant insights.

The first section of the paper presents ten polarimetric principles, arranged in an ordered sequence in which the progression builds on preceding points. Each principle should be obvious in its context, readily supported by the cited references¹. The section that follows comments on the consequences of those ten principles, taken as a whole. Conclusions are offered. The paper includes two Appendices, one that summarizes selected mathematical frameworks supporting the principles, while the second is a brief perspective on quad-pol radar.

2. Ten Essential Elementary Principles

2.1. Power

All quasi-monochromatic electromagnetic (*EM*) fields are comprised of two types of constituents, polarized or unpolarized [Jenkins and White 1957; Born and Wolf 1959]. Total (avg) power I_0 —power scaling—and degree of polarization m —polarized (avg) power allocation—are key interpretive parameters [Wolf 1959; Green 1968].

2.2. Polarimetric ellipticity

All polarized constituents are either linear or circular [Appendix I], which in general combine as a vector sum producing an elliptically polarized *EM* field (Fig 1). The distribution between these two classes of constituents, the magnitude $|\sin 2\chi|$ —ellipticity—is a key parameter.

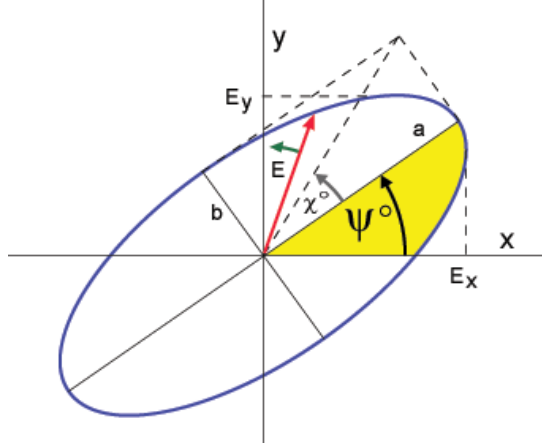


Fig. 1: Polarization ellipse & Poincaré angular variables of the polarized constituents of an *EM* field²

2.3. Sense of circularity

¹While this is a review paper, it includes a useful innovation, summarized in principle *ix*.

²<https://www.nrcan.gc.ca/maps-tools-and-publications/satellite-imagery-and-air-photos/satellite-imagery-products/educational-resources/tutorial-radar-polarimetry/the-polarization-ellipse/9575>

The sense of circularity is reversed with each bounce (each individual reflection³), eventually contributing to the observed *EM* field [Jenkins and White 1957; Green 1968]. The +/- sign of the ellipticity—the R- or L-handed sense of circularity—is a key interpretive parameter [Green 1968; Freeman and Durden 1998; Ostro 2002; Spudis 2013].

2.4. *Three-color rationale*

All backscatter is odd- or even-bounce polarized, or unpolarized [Appendix I]. Hence three primary colors are sufficient to convey nearly all polarimetric information from an observed scene. The corresponding color wheel may be calibrated to quantify combinations of these three backscatter classes. (*NB*: The total power scaling value is also needed. The angle of the dominant linearly polarized constituent [Appendix I] is not included in such three-color schemes, although as may be required it is retrievable from knowledge of the Stokes parameters).

2.5. *Stokes parameters*

Four thoughtfully chosen numbers—the Stokes parameters for example [Stokes 1852; Jenkins and White 1957; Born and Wolf 1959; Hecht 1987]—are necessary and sufficient to fully characterize the polarimetric properties of a partially polarized *EM* field. Claims to the contrary are false.

2.6. *Basis pairs*

A quasi-monochromatic partially polarized *EM* field may be fully characterized by a pair of orthogonally polarized measurements. The Stokes parameters’ measured values do not depend on the specific basis pair with which the *EM* field is observed [Stokes 1852; Jenkins and White 1957; Born and Wolf 1959]. In response to an active system, the observed *EM* field’s polarization properties depend on the polarization of the transmitted illuminating field.

2.7. *Measurement*

For a quasi-monochromatic *EM* field, the Stokes parameters may be evaluated by a coherent dual-polarized observing receiver. “Dual-polarized” requires two orthogonally polarized receive channels (each measuring its averaged signal power), and “coherent” implies measurement of the cross-product of those two signals (the average power of the real and the imaginary parts respectively) [Stokes 1852; Wolf 1954; Jenkins and White 1957; Green 1968; Hecht 1987; Yueh 1997; Robishaw and Heiles 2018]. Those measurements are an example of four numbers—while not themselves Stokes parameters—that are sufficient to fully convey the polarimetric properties of an observed *EM* field.

2.8. *Four canonic parameters*

³Circularity reversal upon reflection is the default condition. When considered in detail, reflection properties of an individual *EM* ray should take into consideration the applicable incident angles and material dielectric properties.

The Stokes parameter measurements can be used to evaluate four canonic parameters [Appendix I], where *canonic* in this context means that the value of each new parameter depends on only one independent variable. The first two canonic parameters denote powers, total I_0 and polarized mI_0 (magnitude scaling and polarized allocation respectively). The other two are the Poincaré angular variables *chi* (χ) and *psi* (ψ) [Hecht 1987] (as visualized in Fig 1, after normalization by mI_0 , after which

$$a^2 + b^2 = 1).$$

2.9. Polarimetric child parameters

Normalization by polarimetric (avg) power mI_0 —in place of the total (avg) power I_0 (which for decades has been the accepted method in radio and radar astronomy)—leads to a canonic circular polarization ratio, revelation of fundamental polarimetric relationships, and the *m-chi* feature classification algorithm [Appendix I].

2.10. Classification methodology

Stokes-based classifications of an observed *EM* field are determined by physics; no model, symmetry, or reciprocity arguments are required [Born and Wolf 1959; Carter et al. 2004; Raney et al. 2012]. This “hands off” “model-free” method is applicable to a wide variety of applications.

3. Consequences

3.1. Polarimetric portraits

A scene’s *polarimetric portrait* [Raney 2021] may be generated from its observed *EM* field *if and only if* the scene is illuminated by *balanced polarization*, which is the essential property of an *EM* field to assure that it has uniform distribution of all linearly polarized constituents. Circular polarization by a radar (or a navigation satellite) satisfies that requirement. In practice, the transmitted field may be elliptically polarized rather than perfectly circularly polarized. This is acceptable once the polarimetric ellipticity has been determined during system calibration.

The conventional quad-pol precedent is to use two interleaved orthogonal polarizations (usually implemented with linearly polarized fields such as H and V). The quad-pol approach achieves polarimetric balance of the illuminating *EM* field, but at the cost of doubling the rate of transmission [Appendix II].

In general, useful multi-purpose polarimetric information cannot be retrieved from a scene that is illuminated by a single linearly polarized *EM* field, no matter its orientation. In specialized applications however, such as weather radar, transmission of a linearly polarized field at 45° orientation with respect to horizontal (known as the slant mode in that application) provides valuable information on hydro-meteors [Bringi and Zrnic, 2019].

3.2. Hybrid Astronomical Radar Polarimeter

A radar astronomical observatory such as the Arecibo Radio Telescope (1964-2020) transmits circular polarization. The backscattered signals are received on two mutually coherent orthogonal channels, usually circularly polarized at the same and opposite sense with respect to the transmitted field, although any pair of orthogonally polarized received constituents would serve the same purpose [Green 1968; Ostro 2002; Raney 2007]. The first two imaging radars in orbit at the Moon—Chandrayaan-1 and LRO [Raney et al. 2011; Misra 2012, Spudis et al. 2013]—were essentially miniaturized embodiments of a conventional radar astronomical instrument. For miniaturized versions of the same architecture, the generic terminology *Hybrid Astronomical Radar Polarimeter (HARP)* is suggested. Chandrayaan-2 (launched in 2019) is equipped with both quad-pol and HARP modes; it is providing data sufficient to compare the lunar geophysical characterization performance of both polarimetric architectures [Bhogapurapu et al. 2021].

3.3. Image classification

Classical radar astronomical image characterization is based on the Stokes parameters, often exploiting child parameters [Appendix I] that serve to reveal selected geophysical properties of the observed scene. The same technique has proven to be effective when applied to data from a HARP-class system for a variety of lunar and terrestrial studies [Carter et al. 2004; Brisco et al. 2020]. Note that conventional quad-pol decompositions [Cloude and Pottier 1996; Moreira et al. 2013] should not be trusted for data collected by a dual-polarized receiver in response to circularly polarized transmissions because only two of the required four scattering matrix element values are known from such measurements, and those two are hybrid parameters, hence the two cross-polarized elements are not symmetric [Emmons and Alexander 1983].

3.4. Calibration

The radar astronomical model—transmitting one circular polarization while receiving (coherently) two orthogonal polarizations such as H and V—is constrained to work with the polarity of the *EM* field that is actually radiated, no matter its imperfections [Brisco 2020]. Since perfectly circularly polarized transmitted *EM* fields are unlikely to be realized in practice, effective calibration is an essential part of any mission that embodies a hybrid astronomical (dual-pol) radar polarimeter. For this class of radar, calibration should be comprised of two steps: *1st* assure that the receiver channels are compensated (within the post-reception signal processor) to be orthogonal, of equal gain, and co-phase; then *2nd* to characterize the transmitted polarimetric *EM* field sufficiently so that it becomes the reference against which polarization deviations in the observed backscatter (relative to that which was transmitted) may be interpreted. The first step requires observation of an external reference source of known polarity [McKerracher et al. 2010] from which the compensation algorithms and parameter values may be determined (standard practice in radio science). For such a radar, any calibration method that is based on knowledge of and corrections to the scattering matrix is destined to fail.

4. Conclusions

Radar polarimetry is a simple concept, a fact that is obscured by quad-pol enthusiasts. Ten fundamental principles capture the essential features of radar polarimetry. Those principles include the fact that only four numbers (the Stokes parameters for example) are sufficient to fully describe the partially polarized properties of an observed scene (whose *EM* emanations are either passive radiation, or reflections in response to active illumination). Those four numbers can be evaluated (without approximation or symmetry assumptions) by an efficient (coherent) dual-pol-on-receiver, be that system either a radar or a radiometer [Raney 2021]. On closer consideration space-based polarimetry gets even simpler.

The Stokes parameter values once measured may be used to evaluate a new set of numbers, the four canonic components of the Poincaré Stokes parameter analytic expressions. Of these, two describe allocation of power (total and polarized), while the other two characterize the (power-normalized) polarimetric portion of the observed scene. Yes, two numbers—not 16 [Appendix II], just the two Poincaré angular variables—are necessary and sufficient to describe the polarized constituents. Only one of those two numbers—*chi*—is of 1st-order importance in response to circularly polarized transmissions.

APPENDIX I: Formal Foundations

AI.1. Stokes parameters

The Stokes parameters are comprised of a set of four numbers. Although their notation takes various forms, their order and respective meanings are invariant with nomenclature. In the following we use

I_o Total power (unpolarized signal, polarized signal, and additive noise)

Q Three independent variables: degree of linearity, polarized power, and orientation of linear pol

U Three independent variables: degree of linearity, polarized power, and orientation of linear pol

V Two independent variables: degree of circularity, and polarized power

Total power includes all constituents, while the other three apply exclusively to the polarized constituents. All four Stokes parameters are real numbers.

AI.2. Stokes parameters—measurement

The value of each parameter may be determined by a dual-polarized receiving instrument [Born and Wolf 1959; Boerner et al. 1998], evaluated by (averaged) sums or differences of observable power-domain measurements. In each case there is only one real number determined for each parameter; each value is independent of the particular pair of orthogonal polarimetric constituents used for the measurement. However, the applicable evaluation formulae depend on the choice of orthogonal polarizations used when observing the received signals.

The backscattered *EM* field observed by a radar is quasi-monochromatic, including both polarized and unpolarized constituents, for which the total power (albedo) I_0 is

$$I_0 = I_U + I_P \quad (1)$$

comprised of the sum of the unpolarized power I_U and the polarized power I_P . These numbers describe the allocation of power between those two basic classes. The polarized power is equal to the root sum of the squares of the polarized constituents

$$I_P = (Q^2 + U^2 + V^2)^{1/2} \quad (2)$$

The unpolarized power I_U includes all uncorrelated contributions, including in particular the system's additive noise along with the unpolarized backscatter constituents.

From these powers, the observed *EM* field's degree of polarization m may be determined

$$m = \frac{(Q^2 + U^2 + V^2)^{1/2}}{I_0}, \quad (0 \leq m \leq 1) \quad (3)$$

which is a parameter of fundamental importance in image characterization [Wolf 1959]. It follows that the polarized portion I_P and unpolarized portion I_U of total power I_0 are given respectively by

$$I_P = mI_0 \quad \text{and} \quad I_U = (1 - m)I_0 \quad (4)$$

where I_0 is the observable.

AI.3. Poincaré Stokes parameters

The measurable Stokes parameters are evaluated according to applicable formulas that rely on directly observable variables. In contrast, the four Poincaré Stokes parameters [Poincaré 1892, Hecht 1987] include two that are directly observable, while the other two require further calculation. Of the two powers, one is directly observable, and the other may be deduced (Eqns 3 and 4). The other two parameters are trigonometric, which are not directly observable quantities. They describe the shape of the observed *EM* field's polarimetric ellipse (Fig 1).

Traditional practice includes normalizing the expressions to minimize (or to remove entirely) the appearance of the power parameters. That practice is unfortunate, as the allocation of power between the polarized and unpolarized constituents is fundamental to the complete polarimetric characterization of an *EM* field. The Poincaré variable expressions (Fig 1) including powers [Hecht 1987] are

$$I_0 = I_0 \quad (5)$$

$$Q = m I_0 \cos 2\psi \cos 2\chi \quad (6)$$

$$U = m I_0 \sin 2\psi \cos 2\chi \quad (7)$$

$$V = m I_0 \sin 2\chi \quad (8)$$

These expressions are used to advantage in the following discussions.

AI.4. Child parameters—traditional total power normalization

Retrievals of specific types of information conveyed by the Stokes parameters are accessed through child parameters [Green 1968; Ostro 2002]. Important examples include:

$$m_l = \frac{\sqrt{Q^2+U^2}}{I_0}, \quad (0 \leq m_l \leq 1) \text{ Degree of linear polarization} \quad (9)$$

$$m_c = \frac{V}{I_0}, \quad (-1 \leq m_c \leq 1) \text{ Degree of circular polarization} \quad (10)$$

$$\text{CPR} = \frac{I_0 + V}{I_0 - V} = \frac{1 + V/I_0}{1 - V/I_0} \text{ Circular Polarization Ratio}^4 \quad (11)$$

These traditional child parameter expressions are power-normalized. Over the past several decades conventional practice has been to normalize by the total power I_0 . Normalization by total intensity I_0 (which includes noise and unpolarized signal constituents) introduces uncertainty, compromises sensitivity, and obscures the underlying physics. We are interested in the information conveyed by the polarized constituents. That suggests that something could be gained through normalization instead by the polarized power I_P .

AI.5. Child parameters—innovative polarimetric power normalization

Polarimetric characterization is the objective. After I_P normalization—expressed in terms of the Poincaré variable *chi* (χ) (Fig 1 and Eqns 5 – 8)—the child parameters are elegant; simple and transparent:

$$m_{Pl} = \frac{\sqrt{Q^2+U^2}}{I_P} = \cos 2\chi, \quad (0 \leq m_{Pl} \leq 1) \text{ **Polarimetric** Degree of linear polarization} \quad (12)$$

$$m_{Pc} = \frac{V}{I_P} = \sin 2\chi, \quad (-1 \leq m_{Pc} \leq 1) \text{ **Polarimetric** Degree of circular polarization} \quad (13)$$

$$\text{CPR}_P = \frac{1 + m_{Pc}}{1 - m_{Pc}} = \frac{1 + \sin 2\chi}{1 - \sin 2\chi} \text{ **Polarimetric** Circular Polarization Ratio} \quad (14)$$

The sign of m_{Pc} indicates odd- vs even-bounce constituents.

AI.6. Canonic Polarimetric Parameters

In distinct contrast to the conventional multi-variable Stokes parameters described in the opening paragraph of this Appendix, the Poincaré expressions embody a new set of four numbers that are sufficient to fully describe the characteristics of an observed partially-polarized EM field. Those numbers are:

⁴The +/- signs in the CPR depend on the circularity handedness of the transmitted EM field. To accommodate the potential ambiguous signage, the usual notation in radar astronomy is SC/OC, referring to the “same sense” (SC) of circular polarization as that which was transmitted, divided by the “opposite sense” (OC), as the expected and usually the stronger return is at the opposite sense as that which was transmitted.

I_o Total power

m Polarized power allocation factor

χ Determines degree of circularity and exposes even/odd bounce heritage

ψ Orientation of dominant linear polarization

These numbers have the great advantage that they are canonic, in the sense that each has only one independent variable. One consequence is that feature characterization ambiguity is minimized, since there is no possibility of cross-talk between the parameters, in contrast to conventional Stokes-based retrievals.

AI.7. Physical Insights

The polarimetric child parameters (Eqns 12, 13) are sufficient to prove basic properties of a partially polarized quasi-monochromatic EM field.

Since the polarimetric degree of circularity must be either positive or negative,

$$m_{\text{Pc}} = \sin 2\chi, \quad (-1 \leq m_{\text{Pc}} \leq 1) \quad (15)$$

shows that all polarized constituents may be characterized by either an odd- or even-bounce heritage.

Since conservation of energy applies to the polarized portion of the *EM* field,

$$m_{\text{Pl}}^2 + m_{\text{Pc}}^2 = 1 \quad (16)$$

shows that all polarimetric fields are blends of linearly and circularly polarized constituents.

The conservation of energy principle (Eqn 16) may be rearranged

$$m_{\text{Pl}} = (1 - m_{\text{Pc}}^2)^{1/2} \quad (17)$$

to show that (i) the polarimetric degrees of circularity and linearity are complementary, and (ii) the polarimetric degree of circularity may be used to evaluate the polarimetric degree of linearity. From this expression, it follows that there is only one number— m_{Pc} —that is the key to describing the polarimetric characteristics of an observed EM field. *NB:* It does not work the other way around, since m_{Pl} cannot be negative, in contrast to m_{Pc} which may be either positive or negative.

These results may be taken one step further. Of the four canonic Stokes-derived variables—under the umbrella of the observed *EM* field’s total power I_o —the dominant polarimetric characteristics of the field may be captured by only two parameters, the degree of polarization m , and the Poincare ellipticity angular parameter χ . (For more on the *m-chi* classification algorithm, see [Raney et al., 2012].) The angle ψ of the dominant linearly polarized constituent may be readily calculated from U/Q (Eqns 6, 7).

APPENDIX II: A Brief on Quadrature Polarimetry

A conventional “fully-polarimetric” polarimeter (and its supporting methodology) measures the four (complex) numbers that comprise the 2x2 (Sinclair) scattering matrix—eight real numbers [vanZyl et al. 1987]. Subsequent analyses [Cloude and Pottier 1996] are usually based on coherence or covariance 4x4 matrices whose 16 elements expose the (averaged) pairwise statistical relationships between the scattering matrix elements.

Measuring all four scattering matrix elements requires interleaved orthogonally polarized transmissions [Burkowitz 1965, p 565; Emmons and Alexander 1983] which means twice as many transmitted pulses per unit time, thus twice as much received data per pixel when compared to a dual-polarized radar that transmits only one polarization. That requirement must be satisfied while respecting the Nyquist sampling rate of the radar [McDonough and Curlander 1992], which is a serious constraint for an orbital system. To satisfy that constraint, the available time between transmissions is reduced by a factor of two which shrinks range coverage by one-half, and it also reduces the total available operation time by another factor of one-half due to spacecraft power constraints. (Alternatively, dynamic digital beam-forming techniques could be exploited to mitigate the range coverage constraint for systems configured to support such a capability [Moreira et al 2013].) Together the range and duration reductions constrict an orbital quad-pol radar’s potential area coverage to be less than one quarter of that of the same instrument’s (dual-polarized) strip-map mode, while doubling the per pixel end-to-end data load, all undesirable attributes for a space mission where power and data capacity are precious limited resources.

Standard quad-pol analysis methodologies reduce the fully-polarimetric 4x4 array—by symmetry and reciprocity arguments—to a 3x3 array [Dubois and Norikane 1987]. Decomposition schemes—of which there are numerous examples having varying degrees of effectiveness⁵—are used to deduce from the input matrix a smaller set of real numbers intended to expose the polarimetric characteristics of the observed scene.

The (averaged) cross-correlations of the scattering matrix elements convey information only about the polarized constituents since the corresponding components of unpolarized backscatter (and additive noise) are not correlated [Cloude and Pottier 1996; Boerner et al. 1998]. It follows that matrix decomposition schemes must reintroduce the allocation of power between the polarized and unpolarized constituents—a key parameter—somehow after the fact.

REFERENCES

- Bhogapurapu, N., Bhattacharya, A. and Y. S. Rao, Y. S. (2021), Chandrayaan-2 Dual Frequency Synthetic Aperture Radar (DFSAR) Full and Compact Polarimetric Data Analysis for the Lunar Surface, *7th Asia-Pacific Conference on Synthetic Aperture Radar (APSAR)*, 2021, pp. 1–5,
doi:10.1109/APSAR52370.2021.9688528.

⁵<https://step.esa.int/main/toolboxes/polsarpro-v6-0-biomass-edition-toolbox/>

- Born, W. and Wolf, E. (1959) *Principles of Optics*; Pergamon Press: New York.
- Boerner, W.-M., Mott, H., Luneburg, E., Livingstone, C., Brisco, B., Brown, R. J. and Paterson, J. S. (1998) "Polarimetry in radar remote sensing: Basic and applied concepts" in *Principles and Applications of Imaging Radar*, vol. 2, F. M. Henderson and A. J. Lewis, Eds., 3rd ed. New York: Wiley, 1998.
- Bringi, V. and Zrnic, D. (2019), Polarization Weather Radar Development from 1970–1995: Personal Reflections. *Atmosphere*, 10, 714, doi:10.3390/atmos10110714.
- Brisco, B., Mahdianpari, M. and Mohammadimanesh, F. (2020). "Hybrid compact polarimetric SAR for environmental monitoring with the RADARSAT Constellation Mission." Special Issue of Remote Sensing on Environmental Mapping Using Remote Sensing, *Remote Sensing*, Vol. 12, p. 3283.
doi.org/10.3390/rs12203283
- Burkowitz, R. S. (1967), *Modern Radar: Analysis, Evaluation and System Design*, J. Wiley and Sons.
- Carter, L. M., Campbell, D. B. and Campbell, B. A. (2004), Impact crater related surficial deposits on Venus: Multipolarization radar observations with Arecibo, *Journal Geophysical Research Planets*, doi:10.1029/2003JE002227
- Charbonneau, F. Brisco, B., Raney, R. K., McNairn, H., Liu, C., Vachon, P., Shang, J., De Abreu, R., Champagne, C., Merzouki, A. (2010), Compact polarimetry overview and applications assessment, *Canadian Journal of Remote Sensing*, 36, S298–S315, doi.org/10.5589/m10-062
- Cloude, S. R. and Pottier, E. (1996), A review of target decomposition theorems in radar polarimetry, *IEEE Transactions on Geoscience and Remote Sensing*, 34(2), 498–518, doi:10.1109/36.485127.
- Cohen, M.H. (1958), Radio astronomy polarization measurements. *Proc. Institute of Electrical Engineers*, 46, 172–181. doi:10.1109/JRPROC.1958.286729
- Dubois, P. C. and Norikane, L. (1987), Data volume reduction for imaging radar polarimetry, *Proc. International Geoscience and Remote Sensing Symposium IGARSS'87*, Ann Arbor, Michigan, IEEE, 691–696.
- Emmons, G. A., & Alexander, P. M. (1983), *Polarization scattering matrices for polarimetric radar* (Technical Report RE-83-1). U. S. Army Missile Command.
- Freeman, A. and Durden, S. L. (1998), "A three-component scattering model for polarimetric SAR data," *IEEE Geoscience Remote Sensing Transactions*, 36, 963–973, doi:10.1109/36.673687.
- Fresnel, A. (1821), "Note sur le calcul des teintes que la polarisation développe dans les lames cristallisées." *Annales de Chimie et de Physique*, Vol. 17, pp. 102–112 (May 1821), pp. 167–196 (June 1821), pp. 312–316 ("Postscript", July 1821).

- Green, P. E. (1968). Radar measurement of target scattering properties (chapter 1). In J. H. Evans, & T. Hagfors (Eds.), *Radar astronomy* (pp. 1–75). McGraw-Hill.
- Hecht, E. (1987) *Optics*, 2nd ed., Addison-Wesley ISBN 0-201-11609-X
- Jenkins, F. A. and H. E. White (1957), *Fundamentals of Optics*, Mc Graw-Hill, New York ISBN-13: 978-0070323285.
- Maxwell, J. C. (1865), "A Dynamical Theory of the Electromagnetic Field", *Philosophical Transactions of the Royal Society of London* 155, 459–512.
- McDonough, R. N. and Curlander, J. C., (1992), *Synthetic Aperture Radar: Systems and Signal Processing*, J. Wiley & Sons, ISBN13:9780471857709.
- McKerracher, P. L., Jensen, J. R., Sequeira, H. B., Raney, R. K., Schulze, R. C., Bussey, D. B. J., Butler, B. J., Neish, C. D., Palsetia, M., Patterson, G. W., Spudis, P. D., and Thomson, B. J. (2010), Mini-RF calibration, a unique approach to on-orbit synthetic aperture radar system calibration. *Lunar and planetary science conference* (p. 2352).
- Misra, Tapan (2012), Where angels fear to tread - The making of RISAT-1, *SAC Courier*, Space Applications Centre, Indian Space Research Organization, 36(3), 2–15.
- Moreira, A., Prats-Iraola, P., Younis, M., Krieger, G., Hajnsek, I. P. and Papathanassiou, K. (2013), A tutorial on synthetic aperture radar, *IEEE Geoscience and Remote Sensing Magazine*, 1(1), 6–43. doi:10.1109/MGRS.2013.2248301. S2CID 7487291.
- Ostro, S. J. (2002), Planetary radar astronomy, *The Encyclopedia of Physical Science and Technology*, 3rd ed., ed R. A. Meyers, 295–328, Academic Press, New York.
- Poincaré, H. 1892. *Théorie Mathématique De La Lumière II. Nouvelles Études Sur La Diffraction*, Paris, France, Gauthier-Villars, p. 306.
- Raney, R. K. (2007), Hybrid-polarity SAR architecture, *IEEE Trans on Geoscience and Remote Sensing*, 45, 3397–3404, doi: 10.1109/TGRS.2007.895883
- Raney, R. K. (2021), Polarimetric Portraits, *Earth and Space Science*, 8, e2021EA001768, doi:10.1029/2021EA001768.
- Raney, R.K., Cahill, J.T., Patterson, G.W., Bussey, D.B.J. (2012), The m-chi decomposition of hybrid dual-polarimetric radar data with application to lunar craters. *Journal Geophysical Research*, 117, E00H21, doi:10.1029/2011JE003986.
- Raney, R. K., Brisco, B., Dabboor, M. and Mahdianpari, M. (2021), RADARSAT Constellation Mission’s Operational Polarimetric Modes: a

User-Driven Radar Architecture, *Canadian Journal of Remote Sensing*, 47(1), doi:10.1080/07038992.2021.1907566.

Robishaw, T. and Heiles, C. (2018), “The Measurement of Polarization in Radio Astronomy”, *arXiv: Instrumentation and Methods for Astrophysics*.

Spudis, P. D., Bussey, D. B. J., Baloga, S. M., Cahill, J. T. S., Glaze, L. S., Patterson, G. W., Raney, R. K., Thompson, T. W., Thomson, B. J. and Ustinov, E. A. (2013), Evidence for water ice on the Moon: Results for anomalous polar craters from the LRO Mini-RF imaging radar, *J. Geophys. Res. Planets*,

doi:10.1002/jgre.20156

Stokes, G. G. (1852), On the composition and resolution of streams of polarized light from different sources, *Trans. Cambridge Philosoph. Soc.*, 9, 399–416.

Tinbergen, J. *Astronomical Polarimetry* (1996), Cambridge University Press (Cambridge, UK),

doi: 10.1017/CBO9780511525100.

vanZyl, J. J., Zebker, H. A. and Elachi, C. (1987), Imaging radar polarization signatures: Theory and observation, *Radio Sci.*, 22, 529–543, doi: 10.1029/RS022i004p00529

Wolf, E. (1954), Optics in terms of observable quantities. *Nuovo Cimento* 12, 884–888,

Doi: 10.1007/BF02781855

Wolf, E. (1959), Coherence properties of partially polarized electromagnetic radiation, *Nuovo Cimento*, 13(6), 1165–1181.

Yueh, S. H. (1997), Modeling of wind direction signals in polarimetric sea surface brightness temperatures, *IEEE Trans. Geoscience and Remote Sensing*, 35(6), 1400–1418, doi: 10.1109/36.649793.